

**NANO PARTICLE REINFORCED LEAD FREE
Sn–3.0Ag–0.5Cu SOLDER PASTE FOR REFLOW
SOLDERING PROCESS**

SRIVALLI A/P CHELLVARAJOO

UNIVERSITI SAINS MALAYSIA

2016

**NANO PARTICLE REINFORCED LEAD FREE Sn-3.0Ag-0.5Cu SOLDER
PASTE FOR REFLOW SOLDERING PROCESS**

by

SRIVALLI A/P CHELLVARAJOO

**Thesis submitted in fulfillment of the requirements
for the degree of
Doctor of Philosophy**

July 2016

DECLARATION

I hereby declare that the work reported in this thesis is the result of my own investigation and that no part of the thesis has been plagiarized from external sources. Materials taken from other sources are duly acknowledged by giving explicit references.

Signature:

Name of student: SRIVALI A/P CHELLVARAJOO

Matrix number: P-CD 0009/14 (R)

Date: 14th July 2016

ACKNOWLEDGEMENTS

One of the most profound learning's of my life is this: the more pain you have to endure on your journey, the sweeter the arrival at your destination; if you want to achieve your highest dreams and overcome your greatest obstacles, prayers is the most powerful medicine that governs the results you seek. I cannot find words to express my gratitude to the ultimate God for blessing me with such a wonderful opportunity to pursue Ph.D program as well completing this research work. I owe my life to God's never ending love and giving me the strength to overcome all the challenges and difficulties I endured throughout this research journey. It gives me great pleasure to appreciate the meditation and yogic power, which really helps me to stay focus and energize all the time.

My road to pursuing the Ph.D program mixed with a little bit of bitterness, hardships and frustration but mostly with trust, encouragement and motivation. It has enriched me with experiences, broadened my knowledge perspective and motivated me to strive for excellence in research. All these were not achieved single-handedly. It will be not enough to express my gratitude in words to those people who helped me, though, I still like to record abundant thanks to all the precious souls for their kind assistance, guidance and support.

Firstly, I would like to express my deepest and sincere gratitude to my honorific supervisor, Professor Ir. Dr. Mohd Zulkifly Abdullah, Dean, School of Aerospace Engineering, Engineering Campus, Universiti Sains Malaysia, for all his valuable guidance and support throughout this research. He patiently supervise and offered me ample of advice to ensure I do not project away from my research scope. His wide knowledge, valuable suggestions, and encouragement have been of

great value for me. I have learned a lot from him and without his backing, I could not have completed my dissertation successfully.

Thereafter, I wish to express my warm and sincere thanks to Dean, Prof. Dr. Zainal Alimuddin Zainal Alauddin, Professor Dr. Mohd Zaidi Mohd Ripin and all the staff of the School of Mechanical Engineering, for their countless efforts and helps in concluding my research work. I would also like to thank Mr. Zambri Samsudin (Sr. Manager-Engineer Technology Services (Asia)), Mr. Yusuf and Mr. Fakhrozi Che Ani (Sr. Advanced Technology Engineer (Asia)) for their support and help to conduct some research work at their industry (Jabil Circuit Sdn. Bhd). Next, I would like to express my appreciation to my ex-colleague, Dr. C.Y.Khor (Senior Lecturer, Faculty of Engineering Technology (FETech), Universiti Malaysia Perlis) for his valuable time and suggestions in discussions.

Then, I gratefully acknowledge my beloved family members for their unwavering love and support. Who am I today is all because the strength in love and care of my parents. I want to express my deepest gratitude to my dear mother Madam Kanagammah and my dear father late Mr. Chellvarajoo for their priceless prayers and inseparable support. I lost my father during my research program. Though, it's a great lost for me, I motivates myself to work harder and give my very best so I could pay tribute to him.

Above all, my loving, supportive, encouraging, and patient husband, Mr. Jeevan Raj whose faithful support during the final stages of this Ph.D is much appreciated. He always has been there for me providing sincere support and encouragement throughout this project work. Furthermore, I would like to convey my sincere and heartfelt thanks to all my family, wherever they are, particularly my

siblings Mr. Balamurugan and Ms. Dehvigah, my family in-laws, and friends who are supported me all the time.

Finally, I am grateful to the Ministry of Higher Education Malaysia (MOHE) for allocating MyBrain15 scholarship to pursue Ph.D studies. Last but not least, I would like to take this opportunity to forward my thanks and appreciation to every individual for their constant supports, encouragements, and helps, directly and indirectly, in accomplishing my dissertation. All good things are worth appreciating and thanking for. Thank you to all beautiful hearts.

Srivalli A/P Chellvarajoo

July 2016

TABLE OF CONTENTS

	Page
ACKNOWLEDGEMENT	ii
TABLE OF CONTENTS	v
LIST OF TABLES	xi
LIST OF FIGURES	xiii
LIST OF ABBREVIATIONS	xxiii
LIST OF SYMBOLS	xxvi
ABSTRAK	xxvii
ABSTRACT	xxix

CHAPTER ONE : INTRODUCTION

1.1 Introduction	1
1.2 Nanotechnology in electronic packaging	2
1.3 Reflow Soldering Process	3
1.3.1 Nano-reinforced solder after reflow soldering process	4
1.4 Reliability of solder joint and Problem Statement	5
1.5 Objectives of the Study	7
1.6 Scope of the research work	8
1.7 Thesis Outline	9

CHAPTER TWO : LITERATURE REVIEW

2.1 Introduction	10
2.2 Solder paste technology	11
2.3 Reliability enhancement of SAC solder alloys	15
2.3.1 Elemental reinforcement into SAC solder	16
2.3.2 Nano-reinforced solder alloys	18

2.4	Melting properties of nano-reinforced solder paste.....	20
2.5	Microstructural analysis for nano-reinforced solder paste.....	21
2.5.1	Intermetallic layer of nanocomposite solders paste	23
2.5.2	Microstructures and nanoparticles displacement of nano-reinforced solder paste after reflow	26
2.6	Mechanical properties of nano-reinforced solders paste	31
2.6.1	Microhardness of nano-reinforced solder paste.....	31
2.6.2	Shear strength of nano-reinforced solder paste.....	32
2.6.3	Tensile strength of nano reinforced solder paste	34
2.7	Wetting properties of nanocomposite solder.....	35
2.8	Conclusions	37

CHAPTER THREE : METHODOLOGY

3.1	Introduction	41
3.2	Preparation of nanocomposite solder paste.....	43
3.3	Differential Scanning Calorimetry (DSC) scan on nanocomposite solder paste for melting behavior analysis	44
3.4	Reflow Soldering Process	47
3.4.1	Copper ‘sandwich’ method.....	51
3.5	Metallographic test	52
3.6	Nano indentation method for hardness measurement.....	53
3.7	Spreading rate and wetting quality analysis.....	53
3.8	Mechanical test for further reliability study.....	55
3.8.1	Shear Test	55
3.8.2	Pull Test.....	60
3.9	Summary	69

CHAPTER FOUR : RESULTS AND DISCUSSION

4.1	Introduction	70
4.2	Effects of Fe ₂ NiO ₄ nanoparticles addition into lead free SAC 305 solder paste.....	70
4.2.1	Melting point.....	77
4.2.2	Microstructure Analysis	80
4.2.2(a)	Intermetallic layer	80
4.2.2(b)	Fe ₂ NiO ₄ nanoparticles motion during reflow soldering process	84
4.2.3	Mechanical properties of solder microstructure using nanoindentation.....	90
4.2.4	Summary for SAC 305-Fe ₂ NiO ₄ nanocomposite solder paste.....	94
4.3	Effects of Diamond nanoparticles reinforcement into lead free SAC 305 solder pastes	95
4.3.1	Melting point.....	96
4.3.2	Microstructure Analysis	99
4.3.2(a)	Intermetallic layer	99
4.3.2(b)	Motion of CN-diamond nanoparticles embedded in nanocomposite solder paste during reflow soldering process	102
4.3.3	Mechanical properties of solder microstructure using nanoindentation.....	104
4.3.4	Summary for SAC 305-Diamond nanocomposite solder paste.....	108

4.4	Effects of NiO nanoparticles reinforcement into lead free	
	SAC 305 solder pastes	108
4.4.1	Melting point.....	110
4.4.2	Microstructure Analysis	113
	4.4.2(a) Intermetallic layer	113
	4.4.2(b) Motion of NiO nanoparticles embedded in	
	SAC 305 solder paste during reflow	
	soldering process	118
4.4.3	Mechanical properties of solder microstructure using	
	nanoindentation.....	119
4.4.4	Summary for SAC 305-NiO nanocomposite	
	solder paste	121
4.5	Effects of γ -Fe ₂ O ₃ nanoparticles addition into lead free	
	SAC 305 solder pastes	122
4.5.1	Melting Temperature.....	123
4.5.2	Microstructure Analysis	126
	4.5.2(a) Intermetallic layer	126
	4.5.2(b) Motion of Fe ₂ O ₃ nanoparticles embedded	
	in SAC 305 solder paste after	
	reflow soldering process	129
4.5.3	Mechanical properties of solder microstructure using	
	nanoindentation.....	133
4.5.4	Summary for SAC 305-Fe ₂ O ₃ nanocomposite	
	solder paste	135

4.6	Effects of ITO nanoparticles reinforcement into lead free SAC 305 solder pastes	136
4.6.1	Melting point.....	137
4.6.2	Microstructure Analysis	139
4.6.2(a)	Intermetallic layer	139
4.6.2(b)	Displacement of ITO nanoparticles reinforced in SAC 305 solders paste after reflow soldering process	142
4.6.3	Mechanical properties of solder microstructure using nanoindentation.....	146
4.6.4	Summary for SAC 305-ITO nanocomposite solder paste	148
4.7	Critical analysis on the effects of different type and sizes of nanoparticle on IMCs	148
4.8	Effects of nano-reinforced solder paste on melting, hardness, spreading rate, and wetting quality.....	151
4.8.1	Melting behaviors and increment in hardness of different nanocomposite solder pastes	151
4.8.2	Effects of different types of nanocomposite solder paste on spreading rate and wetting angle after reflow soldering process.....	155
4.9	Mechanical testing on diamond nanoparticles reinforced solder after reflow	162
4.9.1	Shear test.....	162
4.9.2	Pull test	168

4.9 Summary	173
-------------------	-----

CHAPTER FIVE : CONCLUSIONS

5.1 Conclusions	174
5.1.1 Experimental outcomes	175
5.2 Recommendations for future works.....	178

REFERENCES	179
-------------------------	-----

APPENDICES

Appendix A: Instruments and materials used for experimental works.

Appendix B: Calculation of mean, standard deviation and standard error for parametric tests.

Appendix C: Example of IMCs thickness measurement using Scion Image.

Appendix D: Calculation of spreading rate for SAC 305 solder after reflow.

Appendix E: Custom made PCB.

Appendix F: Detailed Drawing of custom made PCB holder with top cover.

LIST OF PUBLICATIONS

LIST OF TABLES

		Page
Table 2.1	Previous Research works on reinforcement of ceramic nanoparticles in Pb free solder paste.	19
Table 2.2	Effects of various nanoparticles addition into the Pb free solder paste on melting temperature.	22
Table 2.3	Influence in grain size and average spacing of Ag ₃ Sn after nanoparticles reinforcement in SAC alloys.	27
Table 2.4	Wetting properties test for SAC + 4wt.% Ag nanoparticles with various grain sizes at 230 °C (Bukat et al., 2011).	36
Table 2.5	Previous research works in lead free solder paste (SAC305).	39
Table 3.1	Average particle size distribution of nanoparticles via Nanophox with photon cross-correlation spectroscopy.	44
Table 4.1	Solidus, liquidus, and melting range of the Pb free SAC 305 composite solder in this investigation.	78
Table 4.2	Analysis of the elements present in the solder paste by area.	86
Table 4.3	Maximum depth of the indentation tip on the plain solder and composite solder.	93
Table 4.4	Solidus, liquidus, and melting range of the plain solder (SAC 305) and nano composite solder paste (SAC 305-X NiO).	111
Table 4.5	Solidus, liquidus, and melting range of the plain solder (SAC 305) and nano composite solder paste (SAC 305-X Fe ₂ O ₃).	124
Table 4.6	Distribution of Fe nano element in nanocomposite solder after reflow soldering process.	131
Table 4.7	Distribution of elements on top layers of nanocomposite solders (SAC- X wt.% Fe ₂ O ₃) after reflow soldering process.	132
Table 4.8	Solidus, liquidus, and melting range of the plain solder (SAC 305) and nano composite solder paste (SAC 305-ITO).	138

Table 4.9	Microstructure effects after reinforced with different amount of ITO nanoparticles in SAC 305 solder.	144
Table 4.10	Effects of different type and sizes of nanoparticles on IMCs thickness.	151
Table 4.11	Spreading views of various nanocomposite solders on Cu substrate after reflow.	160
Table 4.12	Temperature setting in reflow oven.	170

LIST OF FIGURES

		Page
Figure 1.1	Typical reflow thermal profile (Tsai, 2009).	4
Figure 2.1	Tin-Lead phase diagram (Manko HH., 1992).	12
Figure 2.2	Estimation of Ternary eutectic composition (liquidus surface) (Moon et al., 2000).	15
Figure 2.3	UTS of SAC 305 alloy reinforced with (a) single Co and Ni elements (b) both Ni and Co elements (Cheng et al., 2008).	17
Figure 2.4	(a) FESEM micrograph of cross-sections of SAC 305/Cu interface after reflow (Sujan et al., 2014). (b) Initially formed cross-sections of IMC during SAC 387/Cu solidification process at 231.85°C [Transmission Electron Microscope, (TEM) image] (Gong et al., 2008).	24
Figure 2.5	SEM micrograph of cross-sectional view of SAC 305/Cu interfaces at high aging temperature (150°C) for: (a) 3 days (b) 7 days (c) 21 days (Yoon et al., 2009).	24
Figure 2.6	SEM image of (a) SAC 305 and (b) SAC 305-1.0 wt.% diamond nanoparticles solder interface on Au/Ni-metalized Cu pad after reflow soldering process (Shafiq et al., 2013).	26
Figure 2.7	Scanning Electron Micrograph (SEM) images of microstructure in Sn-3.0Ag-0.5Cu-xTiO ₂ nano-reinforced solders after reflowed: (a) x = 0 wt.%; (b) x = 0.05 wt.%; (c) x = 0.1 wt.%; (d) x = 0.6 wt.% (Tang et al., 2014).	28
Figure 2.8	Microstructure of Ag nanoparticles reinforced SAC 305 solder with various grain sizes [i.e., (a) SAC + Ag3 (137.8 nm); (b) SAC + Ag4 (21.1 nm); (c) SAC + Ag5 (9.3 nm); (d) SAC + Ag5.5 (9.6 nm)] on Cu substrate after reflowed at 250 °C for 30 s (SEM image) (Bukat et al., 2011).	29

Figure 2.9	Microstructure of (a) SAC 305 solder and (b) SAC 305 + 4.0 wt.% micro Ag, on Cu substrate after reflowed at 250 C for 30 s (SEM image) (Bukat et al., 2011).	30
Figure 2.10	Fracture analysis of SAC 305 added with (a, b) 0 wt.% diamond nanoparticles; (c, d) 1% diamond nanoparticles, on Au pad via Scanning Electron Microscopy (SEM) (Fouzder et al., 2011).	34
Figure 2.11	Number of experimental works for different type nanoparticles reinforced SAC 305 solder.	40
Figure 3.1	Experimental investigations on the nanoreinforced lead free Sn-3.0Ag-0.5Cu solder paste for reflow.	42
Figure 3.2	Mechanical mixing.	43
Figure 3.3	(a) Experimental setup for DSC analysis; (b) DSC Standard Cell.	46
Figure 3.4	Stencil design to transfer solder paste on the Cu substrate (a) Schematic design; (b) Actual design.	47
Figure 3.5	Preparation of Copper plate.	48
Figure 3.6	(a) Schematic diagram of experimental setup for thermal profiling; (b) experimental setup in lab scale.	49
Figure 3.7	Setting and experimental reflow profile of infrared lead free reflow oven.	50
Figure 3.8	Solder paste after stencil printing process.	50
Figure 3.9	Copper 'sandwich' sample for FE-SEM analysis.	51
Figure 3.10	Sample preparations for testing: (a) Before epoxy and hardener dried off; (b) After epoxy and hardener dried off.	52
Figure 3.11	Preparations of solder paste for spreading test (a) schematic drawing of disc plate; (b) before solder printing and (c) after solder printing process.	55
Figure 3.12	Solder printing process.	56

Figure 3.13	BGA placement method on PCB via component placement tool.	57
Figure 3.14	Preparation of PCBA for reflow according to appropriate setting of reflow profile.	58
Figure 3.15	Setting and experimental profile of PCBA.	58
Figure 3.16	(a) PCBA during reflow and; (b) Solder joint view before and after reflow.	59
Figure 3.17	Shear test for PCBA.	60
Figure 3.18	Printed Circuit Board with LQFP for pull test.	61
Figure 3.19	Non-contact mixer machine.	62
Figure 3.20	PCB covered with mylar plastic for verifying solder printing.	62
Figure 3.21	Solder printing process.	63
Figure 3.22	Forced-convection reflow oven (Jabil Circuit Sdn. Bhd.).	64
Figure 3.23	Schematic outline of the Surface Mount Technology (SMT) forced convection reflow oven.	65
Figure 3.24	PCB Assembly with thermal profiler.	65
Figure 3.25	Portion of PCB Isolation.	66
Figure 3.26	Mounting of PCB.	66
Figure 3.27	Steel Blot Head.	67
Figure 3.28	Test units after pretreatment.	68
Figure 3.29	Test setup for pull test.	68
Figure 4.1	Morphology of as-received materials (a) Olympus Metallurgical Microscope [MEIJI TECHNO CO., LTD] with computer attachment (b) TEM image of Fe_2NiO_4 nanoparticles.	71

Figure 4.2	(a) Average particle size distribution of Fe_2NiO_4 nanoparticles via Nanophox analyzer; (b) High-resolution transmission electron microscope (HRTEM) image of Fe_2NiO_4 ; (c) XRD micrograph for Fe_2NiO_4 nanoparticles.	72
Figure 4.3	High-resolution scanning transmission electron microscope (STEM) image of SAC 305 solder paste prior to mechanical mixing.	74
Figure 4.4	Elemental mapping on high-resolution scanning transmission electron microscope (STEM) image of SAC 305- Fe_2NiO_4 solder paste: (a) Sn; (b) Ag; (c) Fe; (d) Ni.	75
Figure 4.5	Overall elemental mapping on high-resolution scanning transmission electron microscope (STEM) image of SAC 305- Fe_2NiO_4 solder paste.	76
Figure 4.6	DSC scans for: (a) SAC 305; (b) SAC-0.5 Fe_2NiO_4 ; (c) SAC-1.5 Fe_2NiO_4 ; (d) SAC-2.5 Fe_2NiO_4 .	79
Figure 4.7	Effect of Fe_2NiO_4 nanoparticle reinforcement into the lead free solder paste (SAC 305) on solidus and liquidus temperature.	80
Figure 4.8	FESEM micrographs of cross-sectional view of Sn-3.0 wt.% Ag-0.5 wt.% Cu-x wt.% Fe_2NiO_4 on copper substrate after reflow soldering process: (a) x=0; (b) x=0.5; (c) x=1.5 and (d) x=2.5.	81
Figure 4.9	Fe_2NiO_4 nanoparticles distribution on the β -Sn grain structure for (a) SAC-1.5 Fe_2NiO_4 ; (b) SAC-2.5 Fe_2NiO_4 .	83
Figure 4.10	Effect of different percentage Fe_2NiO_4 nanoparticles addition in SAC 305 on IMCs thickness.	83
Figure 4.11	Schematic diagram of composite solder on copper substrate to clarify the presence of the nanoparticles via copper 'sandwich' method.	85

Figure 4.12	Mobility of nanoparticles from phase A to phase B within copper 'sandwich' layers with the flux during reflow soldering process: (a) SAC 305; (b) SAC-0.5 Fe ₂ NiO ₄ ; (c) SAC-1.5 Fe ₂ NiO ₄ and (d) SAC-2.5 Fe ₂ NiO ₄ .	86
Figure 4.13	Presence of voiding in the composite solder paste (SAC-1.5 Fe ₂ NiO ₄) microstructure on the copper substrate after reflow soldering process (Alicona 3D Optical Microscope): (a) 2-Dimensional view; (b) 3-dimensional view; (c) Depth of the voiding micrograph.	87
Figure 4.14	Presence of voiding in the composite solder paste (SAC-1.5 Fe ₂ NiO ₄) microstructure between the copper 'sandwich' layers after reflow soldering process (Alicona 3D Optical Microscope).	88
Figure 4.15	SEM/EDX analysis of composite solder to differentiate the distribution of nanoparticles around the voiding area and non-voiding area (SAC-1.5 Fe ₂ NiO ₄).	89
Figure 4.16	Nanoindentation marks array with 10mN loads on polished planar surface.	91
Figure 4.17	Ten Indentations to peak loads and displacement at 10mN load rates on the plain solder and composite solders: (a) SAC 305; (b) SAC-0.5 Fe ₂ NiO ₄ ; (c) SAC-1.5 Fe ₂ NiO ₄ and (d) SAC-2.5 Fe ₂ NiO ₄ .	93
Figure 4.18	Effects on hardness after added different percentage of nanoparticles into the SAC 305 solder paste.	94
Figure 4.19	Morphology of as-received materials (a) SEM image of diamond nanoparticles agglomerations (c) XRD micrograph for diamond nanoparticles.	96
Figure 4.20	Average particle size distribution of diamond nanoparticles via Nanophox with Photon Cross-correlation Spectroscopy.	96

Figure 4.21	DSC scans for: (a) SAC 305; (b) SAC-0.5 Diamond; (c) SAC-1.5 Diamond; (d) SAC-2.5 Diamond.	97
Figure 4.22	Effect of Diamond nanoparticles addition into the lead free solder paste (SAC 305) on solidus and liquidus temperature.	98
Figure 4.23	FESEM micrographs of cross-sectional view of Sn-3.0 wt.% Ag-0.5 wt.% Cu-x wt.% diamond nanoparticles on copper substrate after reflow soldering process: (a) x=0; (b) x=0.5; (c) x=1.5 and (d) x=2.5.	100
Figure 4.24	Effect of different percentage diamond nanoparticles addition in SAC 305 on IMCs thickness.	101
Figure 4.25	Displacement of diamond nanoparticles scenario via SEM micrograph and point analysis via Table Top EDX.	104
Figure 4.26	Nanoindentation marks array with 10 mN loads on polished planar surface (SAC 305-0.5wt% Diamond nanoparticles).	105
Figure 4.27	Ten indentations to peak loads and displacement at 10 mN load rates on the plain solder and composite solders: (a) SAC 305; (b) SAC-0.5 wt.% diamond; (c) SAC-1.5 wt.% diamond and (d) SAC-2.5 wt.% diamond.	106
Figure 4.28	Effects on hardness after reinforced different amount of Diamond nanoparticles into the SAC 305 solder paste.	107
Figure 4.29	Morphology of as-received materials (a) FESEM image of NiO nanoparticles agglomerations (b) XRD micrograph.	109
Figure 4.30	Average particle size distribution of NiO nanoparticles via Nanophox with Photon Cross-correlation Spectroscopy.	110
Figure 4.31	DSC scans for: (a) SAC 305; (b) SAC-0.5 wt.% NiO; (c) SAC-1.5 wt.% NiO; (d) SAC-2.5 wt.% NiO.	112
Figure 4.32	Effect of NiO nanoparticle reinforcement into the lead free solder paste (SAC 305) on solidus and liquidus temperature.	113

Figure 4.33	FESEM micrographs of cross-sectional view of Sn-3.0 wt.% Ag-0.5 wt.% Cu-x wt.% NiO nanoparticles on copper substrate after reflow soldering process: (a) x=0; (b) x=0.5; (c) x=1.5 and (d) x=2.5.	114
Figure 4.34	Effect of different percentage NiO nanoparticles reinforcement in SAC 305 on IMCs thickness.	116
Figure 4.35	Scenario of IMCs formation for Sn-3.0 wt.% Ag-0.5 wt.% Cu-x wt.% NiO nanocomposite solder paste during reflow soldering process.	117
Figure 4.36	Top-view morphology of Sn-3.0 wt.% Ag-0.5 wt.% Cu-x wt.% NiO nanocomposite solder paste after reflow soldering process (a) x=1.5; (b) x=2.5.	118
Figure 4.37	Ten indentations to peak loads and displacement at 10mN load rates on the plain solder and composite solders: (a) SAC 305; (b) SAC 0.5 wt.% NiO; (c) SAC wt.% 1.5 NiO and (d) SAC 2.5 wt.% NiO.	120
Figure 4.38	Effects on hardness after reinforced different amount of NiO nanoparticles into the SAC 305 solder paste.	121
Figure 4.39	Morphology of as-received materials: (a) FESEM image of Fe ₂ O ₃ nanoparticles agglomerations; (b) XRD micrograph for Fe ₂ O ₃ nanoparticles.	123
Figure 4.40	Average particle size distribution of Fe ₂ O ₃ nanoparticles via Nanophox with Photon Cross-correlation Spectroscopy.	123
Figure 4.41	DSC scans for: (a) SAC 305; (b) SAC-0.5 Fe ₂ O ₃ ; (c) SAC-1.5 Fe ₂ O ₃ ; (d) SAC-2.5 Fe ₂ O ₃ .	125
Figure 4.42	Effect of Fe ₂ O ₃ nanoparticle reinforcement into the lead free solder paste (SAC 305) on solidus and liquidus temperature.	126

Figure 4.43	FESEM micrographs of cross-sectional view of Sn-3.0 wt.% Ag-0.5 wt.% Cu-x wt.% Fe ₂ O ₃ nanoparticles on copper substrate after reflow soldering process: (a) x=0; (b) x=0.5; (c) x=1.5 and (d) x=2.5.	128
Figure 4.44	Effect of different percentage Fe ₂ O ₃ nanoparticles reinforcement in SAC 305 on IMCs thickness.	129
Figure 4.45	Distribution of nanoparticles analyzed by area.	130
Figure 4.46	Ten indentations to peak loads and displacement at 10mN load rates on the plain solder and composite solders: (a) SAC 305; (b) SAC-0.5 Fe ₂ O ₃ ; (c) SAC-1.5 Fe ₂ O ₃ and (d) SAC-2.5 Fe ₂ O ₃ .	134
Figure 4.47	Effects on hardness after reinforced different amount of Fe ₂ O ₃ nanoparticles into the SAC 305 solder paste.	135
Figure 4.48	Morphology of as-received materials (a) SEM image of ITO nanoparticles agglomerations (c) XRD micrograph for ITO nanoparticles.	137
Figure 4.49	Average particle size distribution of ITO nanoparticles via Nanophox with Photon Cross-correlation Spectroscopy.	137
Figure 4.50	DSC scans for: (a) SAC 305; (b) SAC-0.5 ITO; (c) SAC-1.5 ITO; (d) SAC-2.5 ITO.	138
Figure 4.51	Effect of ITO nanoparticle reinforcement into the lead free solder paste (SAC 305) on solidus and liquidus temperature.	139
Figure 4.52	FESEM micrographs of cross-sectional view of Sn-3.0 wt.% Ag-0.5 wt.% Cu-x wt.% ITO nanoparticles on copper substrate after reflow soldering process: (a) x=0; (b) x=0.5; (c) x=1.5 and (d) x=2.5.	140
Figure 4.53	Effect of different percentage ITO nanoparticles reinforcement in SAC 305 on IMCs thickness.	141
Figure 4.54	Example of EDX Analysis of the IMC layer for ITO nanocomposite solder paste after reflow.	141

Figure 4.55	Displacement scenarios of ITO nanoparticles in SAC 305 solder after reflow soldering.	143
Figure 4.56	Elemental analysis on white spot (Point A1, A2, and A3) for different amount of ITO nanoparticles reinforcement after reflow.	145
Figure 4.57	Ten indentations to peak loads and displacement at 10mN load rates on the plain solder and composite solders: (a) SAC 305; (b) SAC-0.5wt.% ITO; (c) SAC-1.5wt.% ITO and (d) SAC-2.5 wt.% ITO.	146
Figure 4.58	Effects on hardness after reinforced different amount of ITO nanoparticles into the SAC 305 solder paste.	147
Figure 4.59	Effects of different types of nanoparticles on IMCs	150
Figure 4.60	Effects of different type of nanoparticle reinforcement in SAC 305 solder paste on melting behavior.	153
Figure 4.61	Effects of different types of nanoparticle reinforcement in SAC 305 solder paste on hardness behavior.	154
Figure 4.62	Effects of different types of nanoparticle reinforcement in SAC 305 solder paste on spreading rate.	155
Figure 4.63	Effects of different types of nanoparticle reinforcement in SAC 305 solder paste on wetting angle.	156
Figure 4.64	Validation test for height and wetting angle of SAC 305. Cross-section measurement of SEM for (a) angle and (b) height; (c) Alicona's result.	158
Figure 4.65	SAC 305 solder paste after reflow soldering process.	159
Figure 4.66	Shear test sample at printed circuit board assembly after reflow.	163
Figure 4.67	Shear strength of plain solder (SAC 305) and nanocomposite solder joints after reflow.	163

Figure 4.68	SEM fracture surfaces and microstructures after shear test of SAC 305 solder joints doped with Diamond nanoparticles after reflow soldering process; (a and b) 0 wt.%, (c and d) 0.01 wt.%, (e and f) 0.05 wt.%, (g and h) 0.1 wt.%.	164
Figure 4.69	Fracture surfaces of 0.01 wt.% diamond nanoparticles reinforced SAC 305 solder on BGA after shear test.	166
Figure 4.70	Elemental mapping on fracture surfaces of 0.01 wt.% diamond nanoparticles reinforced SAC 305 solder on BGA after shear test.	167
Figure 4.71	Elemental profile plot after line scan analysis of fractured solder joint.	168
Figure 4.72	Example of solder quality inspection after solder printing process.	169
Figure 4.73	Reflow profile for pull test units.	170
Figure 4.74	PCBA views before and after reflow.	170
Figure 4.75	Maximum pull forces of plain solder (SAC 305) and nanocomposite solder joints after reflow.	172
Figure 4.76	The fracture views via (a) SEM and (b) Alicona after pull test (SAC 305-0.01 wt.%).	172

LIST OF ABBREVIATIONS

2D	Two Dimensional
3D	Three Dimensional
Ag	Silver
Al	Aluminium
Au	Gold
BGA	Ball Grid Array
Bi	Bismuth
BSD	Back Scattered Detector
C	Diamond
Ce	Cerium
CN	Carbon Nanostructure
CNT	Carbon Nanotubes
Co	Cobalt
Cu	Copper
DSC	Differential Scanning Calorimetry
EDX	Energy Dispersive X-Ray
EDXA	Energy Dispersive X-Ray Analysis
EPA	Environmental Protection Agency
Fe	Iron
Fe ₂ NiO ₄	Iron Nickel Oxide
Fe ₂ O ₃	Iron (III) Oxide
FE-SEM	Field-Emission Scanning Electron Microscope
Ge	Germanium
H ₂ O	Distilled water

HASL	Hot Air Solder Leveling
HCl	Hydrochloric Acid
HNO ₃	Nitric Acid
HR-STEM	High-Resolution Scanning Transmission Electron Microscope
HR-TEM	High-Resolution Transmission Electron Microscope
IC	Integrated Circuit
IMC	Intermetallic compound
In	Indium
ITO	Indium Tin Oxide
JCPDS	Joint Committee on Powder Diffraction Standards
JEDEC	Joint Electron Device Engineering Council
JIS	Japanese Industrial Standard
LQFP	Low Profile Quad Flat Pack Packages
Mn	Manganese
MpCCI	Mesh-based parallel code coupling interface
MTS	Micro-force Testing System
MWCT	Multi-Wall Carbon Nanotubes
Ni	Nickel
NiO	Nickel Oxide
O	Oxygen
P	Phosphorus
Pb	Lead
PCB	Printed Circuit Board
PCBA	Printed Circuit Board Assembly
Pd	Palladium

Pt	Platinum
RoHS	Restriction of Hazardous Substances Directives
S	Sulfur
SAC	Tin-Silver-Copper
SAC 305	96.5Sn-3.0Ag-0.5Cu
Sb	Antimony
SEM	Scanning Electron Microscope
SMT	Surface Mount Technology
Sn	Tin
TCs	Thermocouples
Ti	Titanium
UTS	Ultimate Tensile Strength
WEEE	Waste from Electrical and Electronic Equipment
XRD	X-Ray Diffraction
Y	Yttrium
Zn	Zinc

LIST OF SYMBOLS

English Symbols

D	Diameter	-
f	Particle volume fraction	-
H	Height of spread solder	mm
n	Constant	-
R	Limiting grain size	-
r	Particle size	-
S_R	Spreading Rate	%
T	Temperature	K
t	Time	s
V	Volume (mass/density of the solder bump)	mm ³
x, y	Cartesian coordinates	-

Greek Symbols

α	constant	-
π	Pi	-
ρ	Density	Kg/m ³

**CAMPURAN PATERI Sn-3.0Ag-0.5Cu TANPA PLUMBUM YANG
DIPERKUATKAN ZARAH NANO UNTUK PROSES PEMATERIAN
ALIRAN SEMULA**

ABSTRAK

Kini penyelidik mula menguatkan pateri tanpa plumbum dengan zarah nano bagi menghasilkan pateri komposit nano berkualiti tinggi. Kajian ke atas campuran pateri yang diperkuat nano dikehendaki oleh jurutera dan penyelidik bagi menyelesaikan masalah pateri terkini dan boleh meningkatkan kualiti sambungan pateri dan merupakan focus bagi penyelidikan ini. Justeru, penyelidikan ini menjalankan kajian kes ke atas perbezaan jenis zarah nano seramik (i.e., oksida pelbagai: Fe_2NiO_4 , ITO; oksida unsur tunggal: NiO, Fe_2O_3) dan zarah karbon struktur nano (CN) (i.e. berlian) sebagai pemboleh-ubah yang dimanipulasikan, digunakan bagi menguatkan aloi pateri SAC 305 secara mekanik. Kesan parameter ini keatas kelakuan lebur, analisis struktur mikro (i.e., ketebalan IMC, pergerakan zarah nano semasa proses pateri aliran semula), kadar serakkan, sudut basah dan kekerasan pateri selepas proses pematerian aliran semula dianalisis. Korelasi diantara pateri yang diperkuat zarah nano dengan beberapa faktor telah dikaji. Ia telah dikenal-pasti bagi campuran pateri diperkuat CN (i.e., berlian) menunjukkan perbezaan ketara dalam kelakuan dan mencapai kekerasan tertinggi, dengan penambahan yang sedikit (i.e., 0.5wt.%) diperkuatkan berbanding dengan jenis zarah nano yang lain. Dengan keputusan ini, zarah nano berlian telah digunakan bagi kajian parameter lanjutan ke atas faktor kualiti (i.e., daya ricih dan tarikan). Kesan daya ricih dan tarikan bagi jumlah perbezaan zarah nano berlian yang digunakan (0.01wt.%, 0.05wt.% dan 0.1wt.%) dengan susuk aliran semula telah dikaji.

Penguatan 0.01wt% zarah nano berlian bagi pateri SAC 305 meningkatkan daya ricih PCBA dan tarikan masing-masing sebanyak 7.4% dan 26.4%. Oleh itu, kajian ini menunjukkan keberhasilan baru keatas CN berdasarkan zarah nano yang diperkuatkan dalam pateri tuang tanpa plumbum bagi meningkatkan kualiti pakej. Zarah nano berdasarkan CN memerlukan hanya sedikit bagi dicampur secara serata dalam pateri tuang SAC 305 dan memberikan peningkatan ketara bagi kualiti sambungan pateri. Tambahan pula, secara tak langsung mengurangkan kos pengeluaran dan memberikan arah berguna bagi jurutera dan penyelidik dalam industri mikroelektronik di masa yang akan datang.

NANO PARTICLE REINFORCED LEAD FREE Sn–3.0Ag–0.5Cu SOLDER PASTE FOR REFLOW SOLDERING PASTE

ABSTRACT

At present, researchers begin to reinforce nanoparticles into Pb free solders to develop high efficiency nanocomposite solders. The effects on nanoparticle reinforcement into SAC 305 after reflow to enhance the solder joint quality are focus of this research. Consequently, this investigation developed into parametric case studies on different type of ceramic nanoparticles (i.e., multielement oxide: Fe_2NiO_4 , ITO; single element oxide: NiO, Fe_2O_3) and carbon-nanostructure (CN) particles (i.e., Diamond) as a manipulated variable (i.e., parameters) which are used to mechanically reinforce into SAC 305 solder alloys, respectively. The effects of these parameters on melting behavior, microstructures analysis (i.e., IMC thickness, nanoparticles motion during reflow), spreading rate, wetting angle and solder hardness after reflow have been analyzed. The correlations between the reinforced nanoparticles with the respective factors have been studied. From this research, it was identified that CN (i.e., Diamond) reinforced solder paste showed unique differences in the behavior and reached highest hardness with very little amount (i.e., 0.5wt.%) of reinforcement among the type of nanoparticles tested. As a result, diamond nanoparticles were used to extend the parametric studies with the mechanical tests (i.e., shear test and pull test). The effects of both shear and pull strengths towards different amount of diamond nanoparticles (0.01wt.%, 0.05wt.% and 0.1wt.%) with respective reflow profile were studied. The addition of 0.01wt.% diamond nanoparticles in SAC 305 solder enhanced the PCBA shear and pull force by 7.4 % and 26.4 %, respectively. Hence, the current study generates a new

expectation on CN based nanoparticles to be reinforced in Pb free solder alloys to enhance package quality. The CN based nanoparticles required in little amount to homogeneously mixed in SAC 305 solder alloys and contribute improvement in solder joint quality. Moreover, it indirectly reduced the production cost and allocates valuable directions for the engineers and researchers in upcoming microelectronics industry.

CHAPTER ONE

INTRODUCTION

1.1 Introduction

The world is embarking on a fast-track in technology transformation. One of the fundamental factors for this was the ever developing microelectronic fields. The evolution of advanced electronic packages well demonstrated via promising reduction in pitch sizes between components and substrates, among components leads-frames, and solder balls arrangements. Hence, the huge jump from wide to narrow space in electronic assemblies greatly influenced the quality of the solder paste. Highly engineered solder technology in the fields of communications, medical, consumer electronics, transportations and industrial, have become the medium for efficient computing demand on the market. The unique solder characteristics with high performance and high quality are needed to be compatible with advanced Ball Grid Array (BGA) and integrated circuit (IC) packages after reflow soldering process. There were still existing solder joint reliability issues for reflow soldering process, this was due to various characteristics of solder alloys. Consequently, researchers and engineers in microelectronic industry attempted to decrease the solder particle size and as well tried adding new particles for solder joint improvement. The modifications and reinforcement process in solder alloys greatly influenced the solder strength. However, the reliability and quality of more advanced packaging assembly was always a concern for the researchers. Therefore, nano-sized particles were introduced in solder paste technology in attempt to tackle these problems. The nano reinforced solder paste improved the quality of the solder joint. During reflow soldering process, in package assembly, the interaction between solder alloys with nanoparticles produced a unique solder joint. The quality of solder joint

also influenced by the characteristic of existing nano alloys. However, the improper combinations of nano sized alloys may yield undesirable defects on solder joint. The poor selection of nanoparticles as reinforcement particles, quantity of alloys, and reflow environment gradually became the roots for package quality failures. Therefore, it is important to understand the scenario happens when different type of nanoparticles reinforced in solder paste during reflow soldering process. The research works on behavior of nano solder, process parameters and material identification for reflow are crucial in solder joint quality enhancement.

1.2 Nanotechnology in electronic packaging

The concept of ultra-small particles or nanoparticles exists over a long duration of time. The American physicist and Nobel Laureate Richard Feynman delivered an inspirational talk entitled, “There’s Plenty of Room at the Bottom” at California Institute of Technology (Caltech) on 1959 (Hornyak et al., 2009). Feynman presented about manipulating the atomic sizes and rearrangements, concept write and read on atomic level, allocate data on a very fine scale, computer miniaturizations, construct fine machines and electronic circuits (Feynman, 1960). The knowledge about the emergence of nanoscale particles founded from Feynman’s notions only a few years later. Nanoparticles defined as extremely small matter that worth one-billionth of a meter (10^{-9} m) per nanometer (Hornyak et al., 2009). The ultrafine particles, or defined as nanoparticles size regime are between 1 to 100 nanometers (nm). As presented by Feynman, the modification, rearrangement, and integration of particles (nanoscale) which create new products that fulfilled industrial and commercial target, was called ‘nanotechnology’. However, the word ‘Nanotechnology’ was first used by Norio Taniguchi in his publication about *On the basic concept of nanotechnology* in 1974 (Taniguchi, 1974). K Eric Drexler

published book *Engines of Creation: The Coming Era of Nanotechnology*, using one of the Feynman's concept in 1986 (Drexler, 1986; Kheiri, 2013). Subsequently, the dramatic advances in the research work on nanoscale were continuously developed in microelectronic field. The microelectronics and electronic devices were scaling down to nanoelectronics. Avouris et al., (2007) stated that the substitution of conducting channel with the carbon based materials (i.e., carbon nanotubes (CNT) or graphene) could enhance the electrical and mechanical properties of the limited size achieved devices. These advanced creation of microelectronic and nanoelectronic devices require higher quality solder paste to be strongly interconnected with substrate or printed circuit board (PCB) after reflow soldering process.

1.3 Reflow Soldering Process

Reflow soldering was an important joining process between surface mount components and PCBs with solder paste to obtain an efficient electromechanical connection (Gao et al., 2008). Smaller sizes of electronic packaging with high efficiency and wide application increase the complexity of reflow soldering process in surface mount technology. The consumption of lead (Pb) free solder paste in reflow soldering process was currently higher than that of Pb based solder paste due to concerning health and environmental issues. Hence, a restricted range of reflow temperature and different melting points of Pb free solders constitute the unique thermal profile of solder paste and the complexity of reflowing on package assembly (Salam et al., 2003; Gao et al., 2008; Florian et al., 2009; Lau et al., 2012a). A unique thermal profile setting of the reflow oven was in the form of temperature versus time, a form that distributes heat and thermal mass in a controlled manner according to the appropriate process time. Four key dominant zones that independently monitor heating rate were generally present in the thermal profile of

reflow soldering process (Figure 1.1). The alteration in duration and temperature of the preheating (zone T1), soaking (zone T2), reflowing (zone T3), and cooling (zone T4) zones greatly influences the quality and reliability of solder joints. Each stage of the reflow thermal profile have an impact on the microstructure and mechanical properties of solder paste due to the varying heat transfer coefficient.

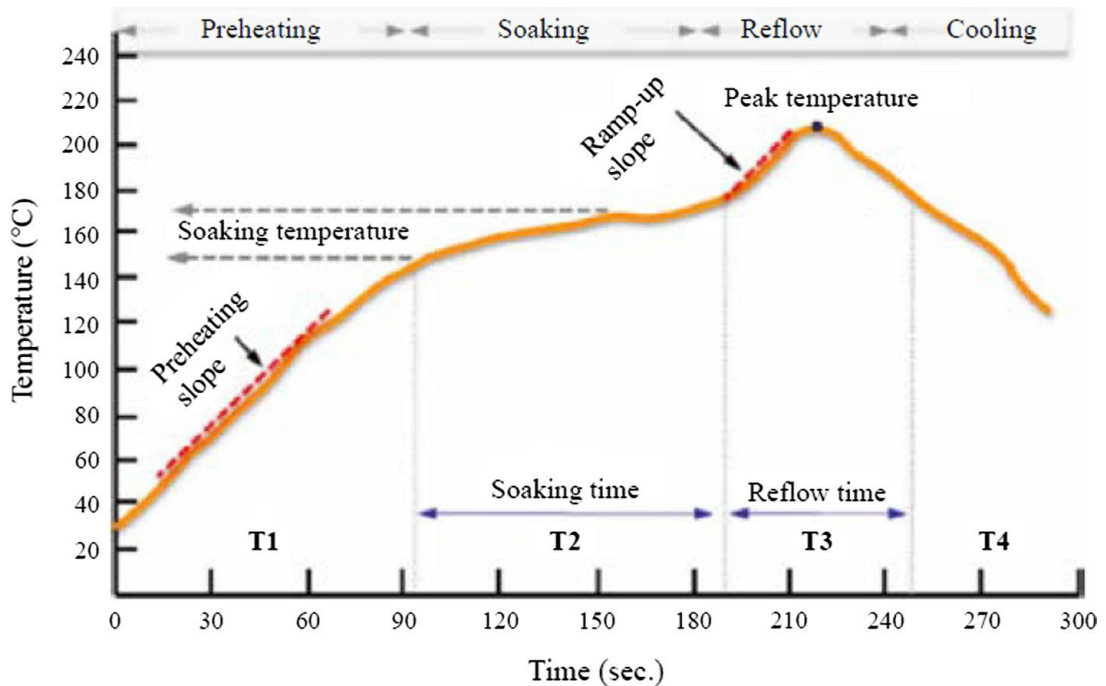


Figure 1.1: Typical reflow thermal profile (Tsai, 2009).

1.3.1 Nano-reinforced solder after reflow soldering process

Solder paste determines the joint strength and thermal, mechanical, and electrical behavior of various electronic packages and substrates. Pb free solder paste was commonly used in electronic packaging industries to eradicate the harmful effects of Pb on human health and the ecosystem (Zhou et al., 2005; El-Daly et al., 2009; Chen et al., 2010; Zhang et al., 2010a; Ervina et al., 2013). Therefore, ternary tin–silver–copper (Sn–Ag–Cu: SAC) solder paste have been selected as a promising replacement material for eutectic tin-lead (Sn–Pb) solder in surface mount application (SMT) (Sujan et al., 2014). Most Pb free solder paste needs higher

thermal energy to melt compared to Sn–Pb solders. Sn-based Pb free low temperature solder alloys have limited applications (e.g., Sn–58Bi: 138 °C; Sn–52In: 118 °C), including heat sensitive packages, because of their expensive raw materials and low reliability. However, Sn–3.0Ag–0.5Cu (SAC 305) solder paste was currently the best option in electronic assemblies for reflow soldering process. SAC 305, a combination of solder alloys, was the preferable and a high-ranked solder paste because of its low cost and effectiveness (Ahmad et al., 2007; Ervina et al., 2013; Sujan et al., 2014). SAC 305 solder paste was commonly applied in SMT, but its quality required improvement (Collins et al., 2012; Kotadia et al., 2014). Therefore, researchers nowadays developed Pb free solder paste that exhibits reliable microstructure (El-Daly and Hammad, 2010), proper intermetallic layer (IMC) growth rate, and suitable melting temperature and mechanical properties (Noor and Singh, 2014). SAC solder paste have been widely tested and improved in terms of quality by adding a small amount of microparticles, such as rare earth, Bismuth (Bi), Antimony (Sb), Iron (Fe), Cobalt (Co), Manganese (Mn), Titanium (Ti), Indium (In), Nickel (Ni), Germanium (Ge), Copper (Cu), and Silver (Ag) (Gao et al., 2010). The particles added to SAC solder slowly shifted from micro-size to nano-size since the electronic packages developed for high-performance applications were also decreased in size. SAC solder alloys reinforced with different types of nanoparticles display unique properties and enhanced quality after reflow.

1.4 Reliability of solder joint and Problem Statement

In microelectronic industries, the quality of a solder joint over long-term usage was an important factor in the production of electronic packages. The higher the reliability of a solder joint, the greater the quality of the electronic product it produce. Solder joint reliability here is defined as the ability of the solder joints to

form strong grip on substrates and sustain under given conditions for a specified period of time without exceeding acceptable failure levels. Even though nanotechnology has been introduced in solder technology for few years now, there were still some limitations in the number of research conducted on nanocomposite solder and nano-material knowledge. This wide research gap was the contributing factor for the obstacles confronted in implementing the nanocomposite solder in the microelectronic industry. Therefore, research on nanoparticles reinforced solder particularly important in yielding better knowledge and understanding on the microstructure and mechanical properties of solder joint for reflow, hence, to be applied in future microelectronic production. Several researches and enhancing activities were carried out by engineers and researchers to analyze the nanoparticulates in solder after reflow. This was due to difficulties to validate the nanoparticle motion throughout solder matrix and its impacts on quality after reflow.

Currently, SAC 305 solder paste was widely used in the microelectronic industries even though there were several question raised on its reliability level. In particular, non-wetting and void formation issues were the uncertainties for SAC 305 solder paste, as these aspects reduce the package reliability in the consequent manufacturing process. The solder wetting process was influenced by physical and process metallurgy. The physical metallurgy defines as the reaction between molten solder on substrate while the process metallurgy describe as the process to make the solder in molten state (Yost et al., 2012). Both metallurgical failures attributed to non-wetting issue. Formation of thicker or no IMCs between solder/substrate interfaces was the example root cause for poor wetting. Poor wetting reduces the effective soldered area and often introduces film defects that can act as strong stress risers, creating subsequent fracture-initiation sites. This poor mechanical

characteristic may lead to failure such as fracture caused by fatigue and void formation after reflow (Choudhury, SF. and Ladani, 2016). The micro-size particles reinforcement as SAC alloy size into Sn-based solder require additional energy and space for the reaction of IMC layer formation and viscosity also increased drastically. Therefore, researchers focused on nanoparticles reinforcement in Sn-based solder to improve the solder joint quality of interconnections. The research works on solders behavior after strengthen the paste through nanoparticles for reflow was crucial to endeavor future problem in microelectronic industry.

1.5 Objectives of the Study

The general objective of this research is to establish alternative Pb free composite solders with new types of nanoparticle reinforcements for reflow soldering process. The understandings of different types of nanocomposite solder behavior after reflow were noteworthy for engineers and researchers as initial steps to improve solder joint quality. In order to accomplish these goals, six primary objectives were focused as indicated below:

1. To formulate appropriate reflow profiles aimed at Cu-solder units for parametric tests and printed circuit assembly units for extended mechanical tests.
2. To establish the effect of different nanoparticles (Fe_2NiO_4 , Diamond, NiO, Fe_2O_3 , ITO) on melting, microstructure and hardness behaviors with respective percentage by weight (i.e., 0.5, 1.5, and 2.5 wt.%) in Pb free solder paste (SAC 305) for reflow.
3. To analyze higher quality nanocomposite solder by measuring melting behavior, solder hardness, spreading rate and wetting angle with the SAC 305 solder.

4. To visualize and identify the nanoparticles motion throughout the SAC 305 solder matrix after reflow.
5. To critically analyzed the effects of different type of nanoparticles on intermetallic compound.
6. To assess the characteristics of the material through the mechanical test (i.e., using shear and pull tests).

1.6 Scope of the research work

In this research study, the reinforcement of new types of nanoparticles in SAC 305 solder paste focused for the solder quality improvement through the experiment. Several type of nanoparticles (i.e., multi element oxide: Iron Nickel Oxide (Fe_2NiO_4), Indium Tin Oxide (ITO); single element oxide: Nickel Oxide (NiO), Iron Oxide (Fe_2O_3); carbon nanostructures: diamond (C)) were reinforced individually in SAC 305 solder with different percentage by weight (0.5, 1.5, and 2.5 wt.%). The preparation methods and analysis techniques of nanocomposite solders remained constant throughout the experimental work for comparative purpose. Consequently, the nanoparticles motion in molten solder during reflow soldering process was identified experimentally. The correlations of all parameters (melting behavior, microstructures and mechanical properties) were analyzed and deduced to identify suitable type and amount of nanoparticles in SAC 305 solder for further mechanical studies. These findings were influential contributions for microelectronic industry.

1.7 Thesis Outline

This thesis is organized into five chapters. In Chapter 1, a brief description about nanotechnology in electronic packaging, reflow soldering process, nanoreinforced solder paste, objectives and scope of research are presented. Then, previous literature works on nanoreinforced solder after reflow is shared in chapter 2. Next, the experimental work flow for the parametric study and quality analysis is highlighted in chapter 3. In chapter 4, the experimental results are analyzed in details and the ideal nanocomposite solder paste with appropriate amount is suggested for reliable solder paste after reflow and extended experimental study. Moreover, the nanoparticles displacement scenarios are discussed for each type of nanoparticles in SAC 305 solder and the correlation of each factor are also described in this chapter. Lastly, concluding remarks on the experimental works and recommendations for the future research are summarized in chapter 5.

CHAPTER TWO

LITERATURE REVIEW

2.1 Introduction

At this moment in time, the microelectronic packaging inclined towards compact, tiny pitch sizes, small lead frames, high performance, higher board density, elevated operation speed, multi-functionality and higher quality. These advanced requirements need high quality solder joint system for rapid response. Researchers and engineers encounter immense challenges in sustaining the solder joint quality improvement via subsequent changes in solder manufacturing process. The changes in solder alloys structures during manufacturing process, for example, substitution, reduction, and reinforcement of particles or alloys plays an important role in solder joint quality enhancement or failure after substantial soldering process. Moreover, the participation of nano-sized particles in solder alloys became current tendency in advanced solder technology. Initially, the effects of size variations on the melting temperature of small particles were experimentally studied by Takagi (1954) (Zou et al., 2010). Consequently, the researches on nanoscale solder in microelectronic industry propagate in early 2000. In this chapter, a significant number of previous literatures on the nanoparticles reinforcement in solder alloys, behavior of different types of nanocomposite solder and displacement of nanoparticles with grain boundaries after reflow soldering process were discussed. Furthermore, the extension tests to determine nanocomposite solder quality were described in detail to identify the research gap for further investigations.

2.2 Solder paste technology

Solder paste behaves as an adhesive to connect leads or terminations of surface mount components with the substrates (Prasad, 1997). Solder paste will be carefully printed on the substrates using stencil with specific design according to the land pattern prior to component placement process. After the stencil was removed, the components were placed on the solder deposits on substrates. The solder strongly bonded between components and substrates via reflow soldering process of surface mount assemblies. A strong and high reliable solder paste with minimum soldering defects for advanced packaging are currently needed in SMT. The quality of solder joint were determined by various factors and process. The solder particle's properties (e.g., size, shape, composition, contents, and mechanical properties) designs were among the significant parameter in determining the solder joint quality and reliability of the final assembly. There are various types of solder paste with different properties currently in use such as, Sn-37.0Pb, SAC alloys, Sn-In, Sn-Bi, Sn-Bi-Ag, Sn-Ag and Sn-Cu.

Pb free solder is a form of Sn-based solder that does not contain Pb element as an alloying material (Japanese Industrial Standard- JIZ 3001, 2003). The characteristics of a tin-lead (Sn-Pb) solder are used as a benchmark for Pb free solder paste that are typically used in the electronic industry for mounting applications. Sn and Pb are group 14 elements in the periodic table; this group exhibits increasing metallic characteristic when going down the group. Therefore, the combination of eutectic Sn-Pb alloys (Figure 2.1) in the solder paste can efficiently decrease the surface tension of pure Sn, forming good IMC compounds (Zhang et al., 2012a), possessed strong mechanical features (Chang et al., 2006), and lastly provide good

connectivity in electronic assemblies with low melting point (Abtey and Selvaduray, 2000; Gao et al., 2010) and low cost (Law et al., 2006).

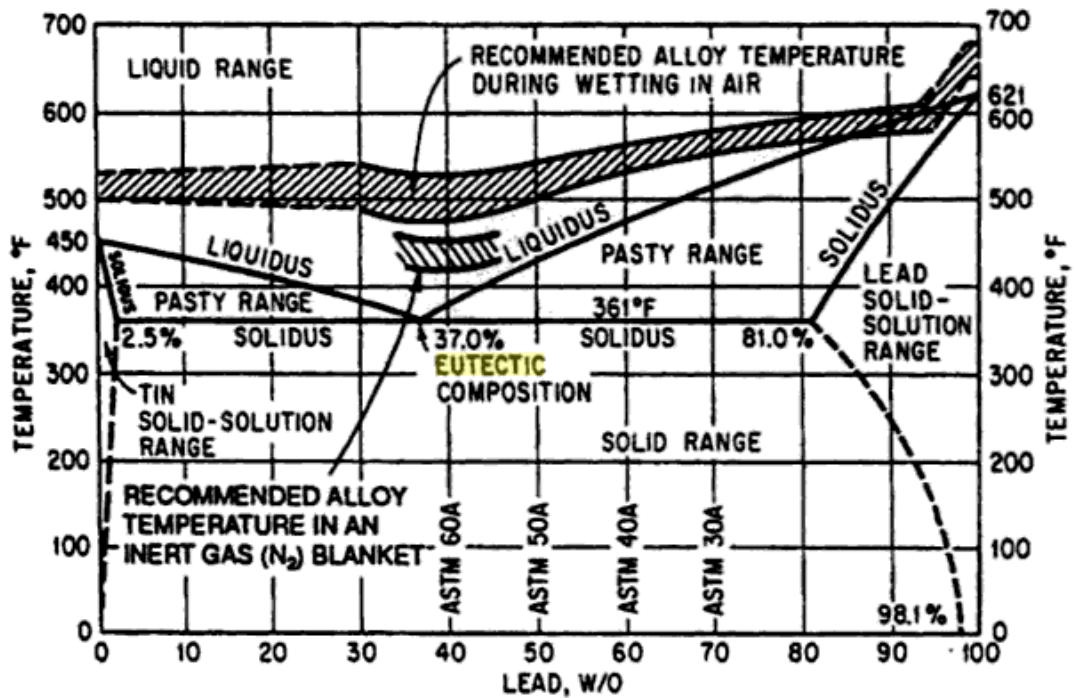


Figure 2.1: Tin-Lead phase diagram (Manko HH., 1992).

Unfortunately, worldwide environmental legislation has banned the use of Pb in solder materials because it contains highly toxic properties that pose serious threats to the ecosystem (Ervin et al., 2013; Zhang et al., 2010; El-Daly et al., 2009; Zhou et al., 2005). The environmentally conscious engineering in electronics committee in Japan, which has stated to normalize the use of Pb free solder from 2003; European legislation under the Waste from Electrical and Electronic Equipment (WEEE); and Restriction of Hazardous Substances (RoHS) Directives, which seriously concern to eradicate Pb use in electronic product by 2006, were the top three legislations that strictly ban on Pb contents in solder paste (Salam et al., 2004). Furthermore, some European countries and Japan had established legislations for recycling Pb content electronic components. Moreover, the environmental protection agency's (EPA) in the United States encouraged the annual report for Pb

usage from electronic manufacturers, and the threshold for Pb consumption was dropped to 100 pounds (Nurmi et al., 2004). As a result, the necessity for Pb free solder paste increased tremendously to substitute widely used Sn-Pb solder in electronic industries. Therefore, the applications of Sn-based lead free solders were established in the blooming of electronic manufacturing as well as product innovation. Especially, the combination of tin-silver-copper (Sn-Ag-Cu; SAC) solder paste is selected as suitable replacements for a Sn-Pb solder (Tay et al., 2011; Yao et al., 2008; Takemoto, 2007; Alam et al., 2003). The thermal, mechanical, and electrical behavior of a Sn-Pb solder are becoming the benchmark for any newly generated Pb free solder paste. The SAC solder paste possess high endothermic energy compared to Pb based solder paste, which means that the temperature required to melt Sn-Pb solders is lower (183°C) compared with SAC ($>200^{\circ}\text{C}$) solder paste (Ervina et al., 2013). Due to lower melting temperature, Sn-Pb solder is still required by few industries to elucidate delamination effects or coefficient of thermal expansion at electronic assembly. However, due to the requirement of 'green products', electronic industries still manage to produce electronic packages that could withstand the thermal load of the Pb free solder paste.

Besides SAC alloy combinations, previously Bismuth (Bi) and Zinc (Zn) were also considered as major alloying partners for Sn solder (Suganuma, 2001; Duan et al., 2004; Islam et al., 2005; Li et al., 2006). However, there were several affects after the addition of different alloys in Sn based solder. Ervina and Singh (2012) carried out experimental investigation on the Sn-9Zn/Copper (Cu) and Sn-4Zn-6Bi/Cu solder alloys. They found that addition of Zn and Zn/Bi into Sn element reduce the melting point of solder to 198°C and 189°C respectively, which were near to eutectic Sn-Pb solder. Sn-9Zn/Cu alloy partner also consists high tensile (30.21

N/mm²) and shear strength (109.00 N/mm²). The addition of Bi increased both tensile and shears strength by 13.7 and 0.9 % respectively, and controlled Zn diffusion process (Mayappan and Ahmad, 2010). Parallel to that, the γ -Cu₅Zn₈ layer formed on the solder/Cu interface weakened the solder joint via transition from ductile to brittle surface (Date et al., 2004). Even though the addition of Zn reduced the manufacturing costs, Zn propagates Kirkendall voids on interface due to diffusivity difference between two different metals. Zn is prone to oxidation and corrosion process. Moreover, if Bi is mixed with Pb elements, the solder strength and fatigue resistance will drop. Consequently, this leads to void formation, cracking and imperfect wetting (Laurila et al., 2005; Tulkoff C., 2011; Zhang et al., 2010a). Above-mentioned stumbling block of Sn based solder instigates unpredictability about preservation, cost and solder joint quality over long term usage.

Hence, after numerous research carried out, electronics industries accepted SAC as the best replacement for eutectic Sn-Pb at the time (Sundelin et al., 2008; Morando et al., 2012; Chuang et al., 2012; Ervina and Singh, 2014). SAC family possessed different types of candidatures with different strength according to the variations in alloy percentages, such as SAC 405 (95.5Sn-4.0Ag-0.5Cu), SAC 357 (95.8Sn-3.5Ag-0.7Cu), SAC 355 (96.0Sn-3.5Ag-0.5Cu), SAC 387 (96.5Sn-3.8Ag-0.7Cu), SAC 305 (96.6Sn-3.0Ag-0.5Cu), SAC 105 (98.5Sn-1.0Ag-0.5Cu) and SAC 0307 (99.0Sn-0.3Ag-0.7Cu). The phase diagram for Sn rich ternary eutectic compositions is shown in Figure 2.2. It shows the relationship of SAC microstructure reactions towards thermal loads. Phase diagram also helps in near eutectic candidature selection process for package assembly (Kattner, 2002). SAC 305 candidate is widely chosen as a dominant and standard soldering material among the Sn-based solders because of its acceptable melting temperature, availability, cost and

performance effectiveness (Ahmad et al., 2007; Ervina et al., 2013). Unfortunately, challenges encountered when Sn-based solders containing binary or ternary alloys are used. Nowadays, researchers recognized the use of SAC 305 in electronic assemblies also contributed to fragility, void formation, wetting issues, process temperature issues, and fatigue issues, which were predominant failure mechanisms for solder joint reliability (Collins et al., 2012; Kotadia et al., 2014). Solder joint failure could lead to electronic products failure. Thus, researchers continually conduct investigations to further develop the efficiency of SAC solder paste after reflow soldering process.

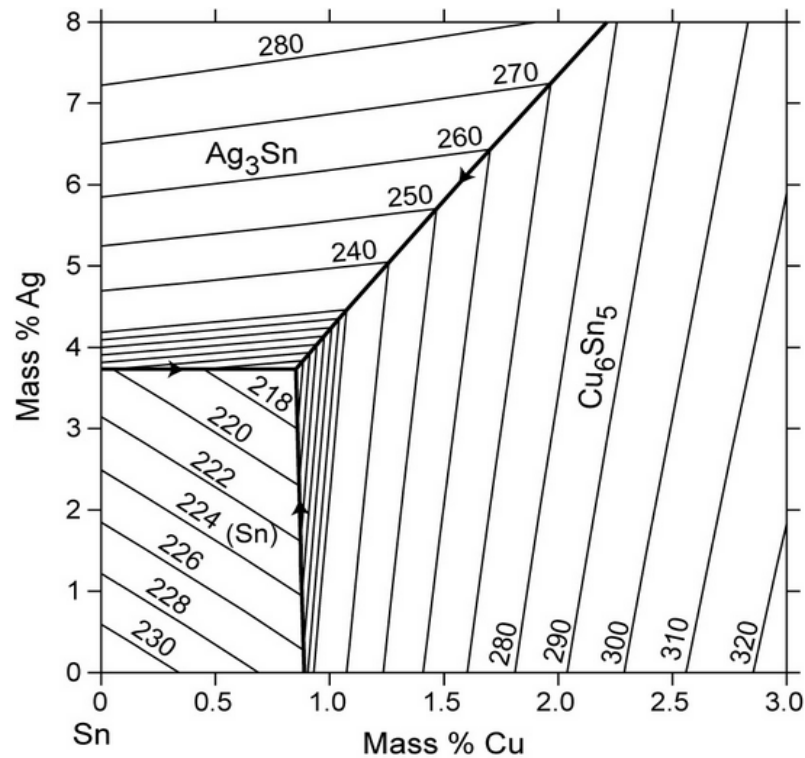


Figure 2.2: Estimation of Ternary eutectic composition (liquidus surface) (Moon et al., 2000).

2.3 Reliability enhancement of SAC solders alloys

The chemical reactions between solder alloys compositions and reinforced particles, resulted in unique microstructures that contribute either positive or negative influences in solder mechanical properties. Additionally, the grain boundaries

displacement in-between solder microstructures with different mechanical characteristics affect the solder quality.

2.3.1 Elemental reinforcement into SAC solder

Researchers reinforced various particles such as Mn, Ti, Y, Bi, Ce, Ni, Co, Pt, Fe, Zn, Ni, Sb, Al and rare earth Yb into the SAC solder paste to enhance its interconnection reliability (Billah et al., 2014; Fallahi et al., 2012; Lee et al., 2008; Zhang et al., 2014). The reinforcement of these alloying elements resulted in discernible changes in the state-of-the-art Pb free composite solder paste, especially on the interfacial IMCs, solidification process and mechanical properties (Kotadia et al., 2014). Laurila et al. (2010) classified the alloying elements to two different categories based on the reactivity towards IMCs via thermodynamic–kinetic method. The elements in first group were Ni, Au, Sb, In, Co, Pt, Pd, and Zn which involved in the interfacial reaction mechanism. Meanwhile, Bi, Ag, Fe, Al, P, rare-earth elements, Ti, and S were dropped in second group which act as ‘catalyst’ in the IMC formation scenario and not involved themselves in the reaction process. Cheng et al. (2008) also identified that addition of both Ni and Co elements into SAC 305 solder alloys initiates the presence of CoSn_2 IMCs which leads to micro cracks and ductility reductions. There were only small changes in the ultimate tensile strength (UTS) of SAC 305 solder matrix after added with Ni, Co and both Ni/Co elements as indicated in Figure 2.3.

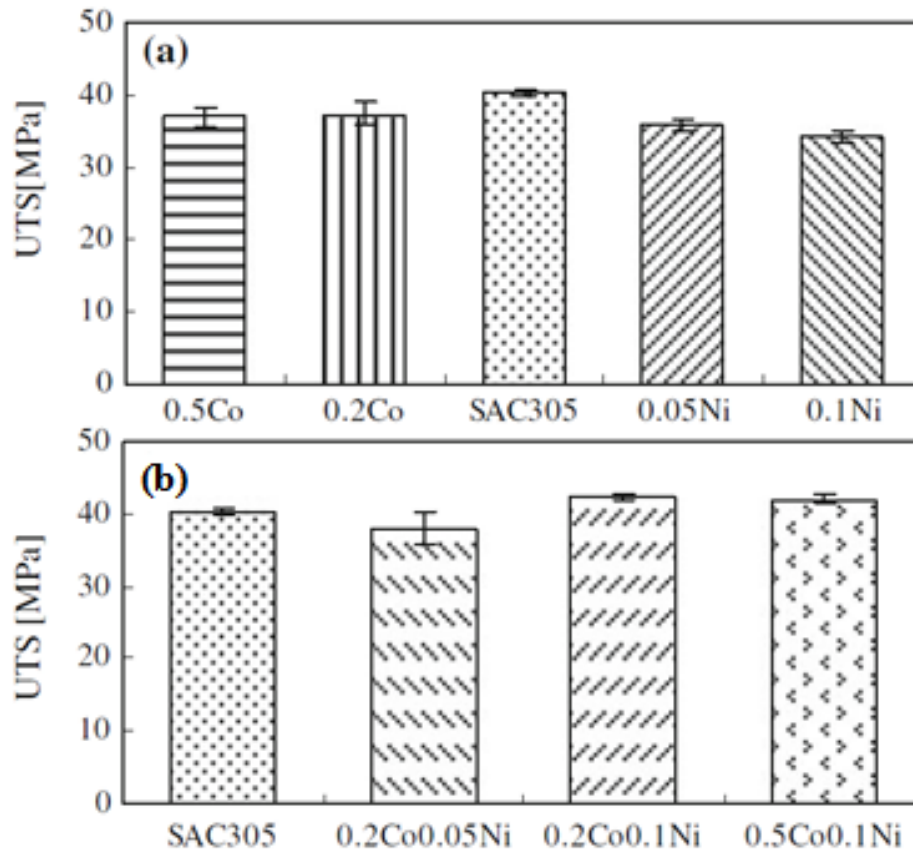


Figure 2.3: UTS of SAC 305 alloy reinforced with (a) single Co and Ni elements (b) both Ni and Co elements (Cheng et al., 2008).

Xia et al. (2002) found that the addition of Ag, Bi and rare earth elements to pure Sn reduced the growth rate of IMCs and increased the tensile strength in the range of 40 to 50 % respectively. Micro-sized particles, such as 0.2 wt.% of Zn, were added into Sn-based solder to reduce the void formation on the Cu_3Sn layer between the $\text{Cu}_6\text{Sn}_5/\text{Cu}$ substrate (Kotadia et al., 2014). The reinforcement of alloying elements should not exceed the limits to avoid reduction in solder quality. There were failure in drop test performance when the reinforcement of Ni and Co elements into SAC is more than 0.1 wt.% (Laurila et al., 2010). So, the overall consideration on microstructures, IMCs, mechanical strength and failure of solder paste were very important to surmount reliability issues. The homogeneous particle size reinforcement as SAC alloy size into Sn-based solder needed more energy and

interval in the reaction of IMC layer formation and viscosity also enhanced significantly. Consequently, the transfer efficiency of solder paste through stencil also dropped since the advanced electronics components are getting into ultra-fine pitch interconnections. Therefore, researchers focused on nanoparticles reinforcement in Sn-based solder to enhance the interface stability of interconnections. Ervina and Singh (2014) stated the variations between micro and nanoparticles reinforcement in solder system. The added micro elements in the solder are diffused as another alloy. However, the nano scale particles behaved as discrete matter in the solder matrix. Hence, the distinct nanoparticles behavior in solder system begins diverse researches on nano-reinforced solder properties for enhanced solder joint quality.

2.3.2 Nano-reinforced solder alloys

SAC solder alloys reinforced with different types of nanoparticles display unique properties and enhanced solder quality. The nanoparticles reinforcements alter the melting behavior; microstructures and interfacial characteristics; mechanical properties; spreading rate and wettability of growing nanocomposite solder system. All these are key factors in identifying and developing a reliable nanoreinforced solder paste to fulfill electronic manufacturing demand. Nano-reinforced solder paste were prepared by several methods such as manual mixing (Haseeb and Leng, 2011; Haseeb et al., 2012), mechanical reinforcement (Liu et al., 2008; Tai et al., 2010), and chemical reduction process (Lin et al., 2009; Zou et al., 2010). If nanoparticles homogeneously mixed with solder alloys, the modified nanocomposite solder paste clearly showed various changes in properties compared to reference solder paste. Basically, particle size increment in solder matrix may attribute to the increment in melting temperature (Shen and Chan, 2009b; Gao et al., 2009; Zou et al., 2010). Zou

et al. (2010) experimentally proofed that the chemically reduced SAC 305 nano solder alloys which in the range 80 to 100 nm, reduced the melting temperature of reference SAC 305 (217.8°C) by 1.4 to 1.9 %. The size dependent thermal effect revealed that nanoparticles possessed large surface area per unit volume which instable at low temperature. Hence, the nano alloys tends to reduce the melting temperature. In the case of nano-reinforced solder paste, the thermal characteristics of solder were dependent on properties and amount of nanoparticles reinforcement as described in section 2.4. The existence of strong bonding or pinning between nanoparticles and solder alloys plays a significant role in mechanical properties improvements. There was several research works conducted on various types nanoparticle reinforced SAC solder properties with different percentage (%) of reinforcements as shown in Table 2.1.

Table 2.1: Previous Research works on reinforcement of ceramic nanoparticles in Pb free solder paste.

Pb free solder paste (SAC)	Nanoparticles reinforcement (wt.% of addition)	References
Sn-3.0Ag-0.5Cu	TiO ₂ (0.02, 0.05, 0.1, 0.3, 0.6, 1.0)	Tang et al., 2013 & 2014; Gain et al., 2011c.
	ZrO ₂ (0.5, 1.0, 3.0)	Gain et al., 2011& 2011d.
	Y ₂ O ₃ (0.1)	Yang and Zhang, 2013.
	Trace Diamond (0.5, 1.0, 1.5)	Shafiq et al., 2013.
	Multi-walled Carbon Nanotubes (0.01, 0.05, 0.1, 0.5)	Bukat et al., 2012 & 2013.
Sn-3.5Ag-0.25Cu	TiO ₂ (0.25, 0.5, 1.0)	Tsao et al., 2010.
Sn-3.5Ag-0.5Cu	SrTiO ₃ (0.5)	Fouzder et al., 2011.
	TiO ₂ (0.25, 0.5, 1.0)	Chang et al., 2011; Chuang et al., 2012.
	Al ₂ O ₃ (0.25, 0.5, 1.0)	Tsao et al., 2010 & 2013.
	Multi-walled Carbon Nanotubes (0.01, 0.05, 0.1)	Xu et al., 2014.
Sn-3.8Ag-0.7Cu	Co (0.5, 1.0, 1.5, 2.0)	Haseeb and Leng, 2011; Tay et al., 2011.
	Mo (1.0, 2.0, 3.0)	Haseeb et al., 2012.
	SiC (0.01, 0.05, 0.2)	Liu et al., 2008.
	Ni (0.5, 1.0, 1.5, 2.0)	Tay et al., 2013.
	Zn (1.0, 2.0)	Chan et al., 2013.

2.4 Melting properties of nano-reinforced solder paste

Melting temperature plays an important role in the selection process of newly manufactured nano-reinforced solder paste with good joint quality. Melting temperature is another form of liquidus temperature (liquidus, T_L). The liquidus temperature state is achieved when the solder alloys are completely in molten state. Hence, the effort to produce and improve nano-reinforced solder paste with melting temperature near eutectic Sn-Pb solder, is another concerns in the electronic industry. Parallel to T_L , solidus temperatures (T_S) also influence the solder joint quality (Mei et al., 1996; Kanlayasiri et al., 2009). The solidus temperature is the maximum temperature that a solder alloy remains in its solid form. This temperature has a significant effect on the microstructure and grain size of a solder alloy. Table 2.2 shows the effect of adding various amounts of nanoparticles into a SAC solder paste at solidus and liquidus temperatures. The results from previous literature revealed that the reinforcements of nanoparticles slightly change the solidus and liquidus temperature compare to standard SAC. Chang et al., (2011) found that the addition of 0.5 wt.% of TiO_2 nanoparticles to the SAC 357 solder increased the melting range by 64.1 %. Likewise, Gain et al., (2011) identified that reinforced 0.5, 1.0 and 3.0 wt.% of ZrO_2 nanoparticles in SAC 305 solder enhanced the melting range by 7.0, 4.7 and 9.3%, respectively. However, the slight increment in the melting range does not contribute harmful affect towards solder quality (Ervina and Singh, 2014). Overall, the melting range increases with the reinforcement of nanoparticles, except for $SrTiO_3$, into the SAC. Therefore, the characteristics of the element in the specific nano powders affect the thermal properties of the particular composite solder paste. Moreover, the density differences between the elements present in the nanoparticles

varied in the SAC solder paste. Therefore, during the reflow soldering process, there is a high rate of movement in nanoparticles which influence the properties of solders.

2.5 Microstructural analysis for nano-reinforced solder paste

The microstructure design of solder matrix determines the solder/substrate joint strength (El-Daly, AA, and Hammad, 2010; Garcia et al., 2010; Osorio et al., 2013). The homogeneously distributed solder alloys with fine structure morphology is crucial for quality enhancement (Roubaud et al., 2001; Shen and Chan 2009a). The reinforcements of nanoparticles in SAC altered the physical properties of the solder microstructures formed. The average grains sizes and spacing of the solder structures are continuously reduced with the reinforcement of nanoparticles into SAC (Chang et al., 2011; Tsao et al., 2012). Additionally, the interactions between molten solder alloys with substrate after reflow soldering process initiated chemical reactions that produced intermetallic compound between solder and substrate (Mayappan and Ahmad, 2010). The characteristics of reaction products varied based on the solder compositions and substrates types (Abtey and Selvaduray, 2000). There were advantage and disadvantage in the existence of IMC layer. The growth of thin IMC layer upgrades the solder strength; whereas the excessive thick IMC degrades the solder quality (Zou et al., 2010; Ervina et al., 2013). The thick IMC layer consisted with brittle structure which propagates cracks and finally failed to form joint. However, majority of previous works clarified that the reinforcement of nanoparticles such as ZrO_2 (Gain et al., 2011; Shen and Chan, 2009a), TiO_2 (Chang et al., 2011), multiwall carbon nanotubes (MWCT) (Bukat et al., 2012; Bukat et al., 2013) and Mo (Haseeb et al., 2012) in Sn based solder matrix successfully reduced the growth rate of IMC layer. These microstructural properties indirectly influenced the mechanical properties and hence, the quality of nano-reinforced solders paste.

Table 2.2: Effects of various nanoparticles reinforcement into the Pb free solder paste on melting temperature.

Lead free solder paste	Reinforced nanoparticles (wt.% of addition)	Findings				References
		Materials	T _S (°C)	T _L (°C)	ΔT (°C)	
Sn-3.5Ag-0.7Cu	Titanium dioxide, TiO ₂ (0.5)	SAC	217.3	221.2	3.9	Chang et al., 2011.
		SAC-0.5TiO ₂	217.7	224.1	6.4	
Sn-3.5Ag-0.5Cu	Aluminium oxide, Al ₂ O ₃ (0.25, 0.5 and 1.0)	SAC	217.7	221.2	3.5	Tsao et al., 2010.
		SAC-0.25Al ₂ O ₃	217.4	222.3	4.9	
		SAC-0.5 Al ₂ O ₃	217.4	222.7	5.3	
		SAC-1.0 Al ₂ O ₃	217.4	223.0	5.6	
Sn-3.0Ag-0.5Cu	Zirconia, ZrO ₂ (0.5, 1.0 and 3.0)	SAC	217.0	221.33	4.3	Gain et al., 2011.
		SAC-0.5ZrO ₂	217.08	221.63	4.6	
		SAC-1.0 ZrO ₂	217.12	221.65	4.5	
		SAC-3.0 ZrO ₂	217.25	221.95	4.7	
Sn-3.8Ag-0.7Cu	Silicon Carbide, SiC (0.01, 0.05 and 0.2)	SAC	-	219.9	-	Liu et al., 2008.
		SAC-0.01SiC	-	219.2	-	
		SAC-0.05SiC	-	219.0	-	
		SAC-0.2SiC	-	218.9	-	
Sn-3.8Ag-0.7Cu	Cobalt, Co (0.5, 1.0, 1.5, and 2.0)	SAC	216.31	-	-	Tay et al., 2011.
		SAC-0.5Co	217.68	-	-	
		SAC-1.0Co	217.85	-	-	
		SAC-1.5Co	217.58	-	-	
		SAC-2.0Co	217.70	-	-	
Sn-3.0Ag-0.5Cu	Strontium titanate or rhodium, SrTiO ₃ (0.5)	SAC	217.00	221.33	4.3	Fouzder et al., 2011.
		SAC-0.5SrTiO ₃	217.66	221.53	3.9	

Notes: T_S (°C)-solidus temperature; T_L (°C)-liquidus temperature; ΔT (°C)-temperature range.

2.5.1 Intermetallic layer of nanocomposite solders paste

IMC is a unique layer that forms between molten solder and the substrate during the reflow soldering process. Reflow soldering has a very crucial function in joining the surface mount components with the PCB and in determining the highest integrity of the solder joint (Illés, 2010, Masood and Srihari, 1990). The IMC founds between SAC solder and Cu substrate was Cu_6Sn_5 , Cu_3Sn and Ag_3Sn (Zhang et al., 2012a; Gong et al., 2008 & 2009; Yoon et al., 2009; Anderson et al., 2001). Gong et al. (2008) identified that the Cu_6Sn_5 - Cu_3Sn -Cu layers forms between molten SAC interface and Cu substrate during liquid/solid transformation phase. The experiments conducted by Sujana et al. (2014) also supported the formation of layers at SAC 305/Cu interface (Figure 2.4). However, the thickness of each layers influenced by reflow profile, dwell time and heterogeneous alloys or particles dissolutions. Additionally, Yoon et al., (2009) clarified that the Cu_3Sn grows faster than Cu_6Sn_5 layer at high aging temperature on interface SAC 305/Cu as shown in Figure 2.5. The presence of nanoparticles in between SAC solders paste and Cu substrates greatly affect the formation of IMCs.

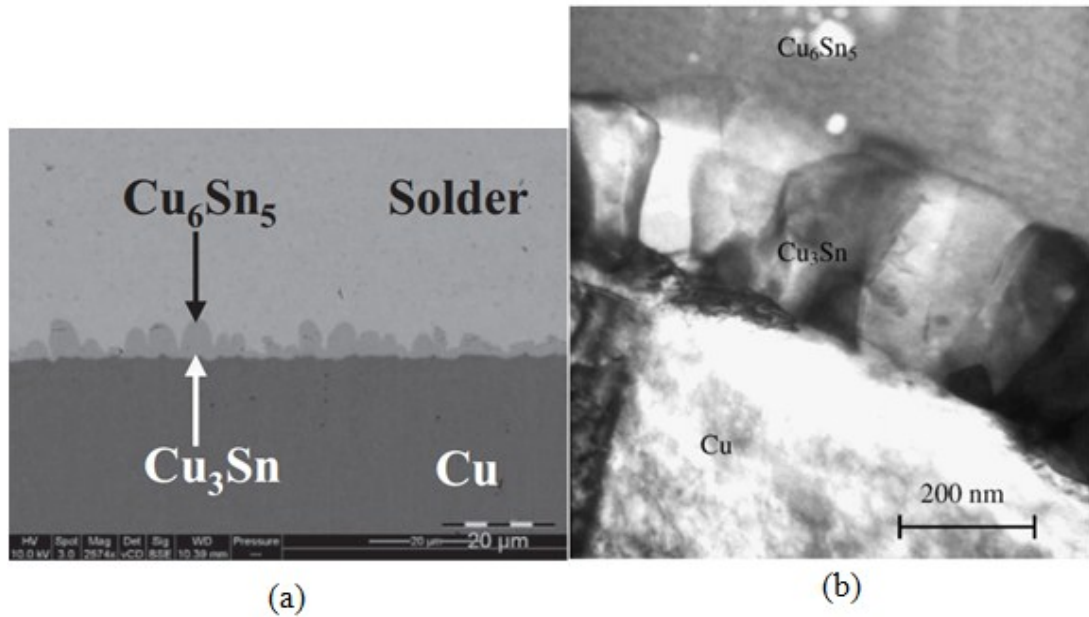


Figure 2.4: (a) FESEM micrograph of cross-sections of SAC 305/Cu interface after reflow (Sujan et al., 2014). (b) Initially formed cross-sections of IMC during SAC 387/Cu solidification process at 231.85°C [Transmission Electron Microscope, (TEM) image] (Gong et al., 2008).

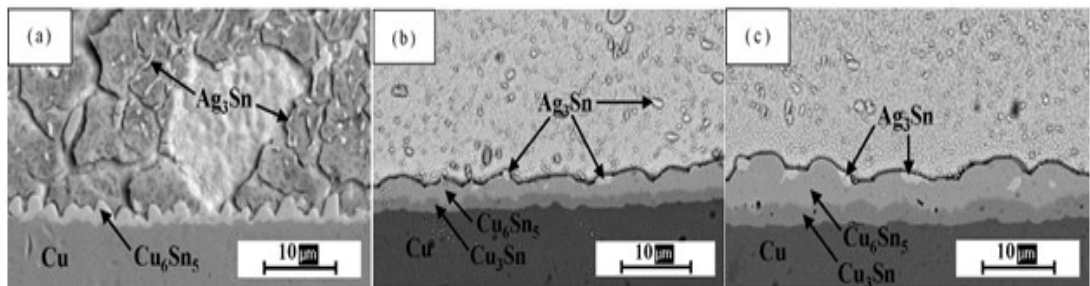


Figure 2.5: SEM micrograph of cross-sectional view of SAC 305/Cu interfaces at high aging temperature (150°C) for: (a) 3 days (b) 7 days (c) 21 days (Yoon et al., 2009).

Tang et al., (2013) found that the IMC growth significantly reduced with the increment in percentage of TiO_2 nanoparticles in SAC 305 solder paste on Cu pad. After reached 0.1 wt.% TiO_2 in SAC 305, the IMC growth rate slightly increased. The TiO_2 nanoparticles adsorbed into molten solder matrix and act as a ‘catalyst’ in the formation of Cu_6Sn_5 IMC as mentioned in Section 2.3.1. Similar scenario for the Cu_6Sn_5 IMC formation at the interface described as heterogeneous nucleation by Tang et al., (2013). The nanoparticles actively inhibit the elemental diffusivity